

Potassium bromide, KBr/ε : New Force Field

Raúl Fuentes-Azcatl* and Marcia C. Barbosa*

*Instituto de Física, Universidade Federal do Rio Grande do Sul, Caixa Postal 15051, CEP
91501-970, Porto Alegre, RS, Brazil*

E-mail: razcatl@hotmail.com; marcia.barbosa@ufrgs.br

*To whom correspondence should be addressed

Abstract

A force field needs to reproduce coincident many properties of ions, like their structure, solvation, and moreover both the interactions of these ions with each other in the crystal and in solution and the interactions of ions with other molecules. Using a similar strategy employed in the parameterization of the NaCl/ ϵ ,⁸ in this paper, we first propose a force field for the Potassium Bromide, the KBr/ ϵ . This new model is compared with the experimental values of cristal density and structure for the salt and the density, the viscosity, the dielectric constant and the solubility in the water solution for a range of concentrations. Next, the transferability, of this new model KBr/ ϵ and the NaCl/ ϵ , is verified by creating the KCl/ ϵ and the NaBr/ ϵ models. The strategy is to employ the same parameters obtained for the NaCl/ ϵ and for the KBr/ ϵ force fields. The two new models derived are also compared with the experimental values for the density, the viscosity, the dielectric constant and the solubility in the water solution for a range of concentrations.

Introduction

The potassium Bromide salt shows a number of applications in medicine particularly in the metabolic regulation.¹ The potassium levels influence multiple physiological processes, including¹⁻³ the cellular-membrane potential, the propagation of action potentials in neuronal, in the muscular, and in the cardiac tissue. Recent studies suggest that bromine is necessary for tissue development⁴⁻⁶ and is relevant in the antiparasitic enzyme in the human immune system.

The salt interaction with the biological system is quite complex and experiments even though very important are unable to isolate the properties of the individual molecule-molecule interaction. Therefore, one strategy to understand the interaction of the KBr with other molecules is the use of simulations. The crucial step in the simulations is to construct an appropriated force field for the interaction potential between the ions. The usual method

is to fit the parameters of the model with the experimental results for the density and for the structure for the real system at one determined pressure and temperature. Then, the results obtained for thermodynamic and dynamic properties with the model are compared with experiments. Following this procedure, atomistic models for KBr have been proposed.⁷ Unfortunately, even though capable of reproducing the density of the system at 298K and 1bar the current models fail in reproducing other properties such as the the dielectric constant of the solution in water, the viscosity and the solubility.

Recently we proposed a new model for Sodium Chloride,⁸ the NaCl/ ϵ , which is able to reproduce not only the density, but the dielectric constant, the viscosity and the solubility of this salt in aqueous solution, as well as, the density of the pure system at different temperatures. The idea of adjusting the model to give the experimental dielectric constant of the pure system and of the water solution at 1bar and 298K is inspired by the recent need to understand the behavior of salt in surfaces and confined geometries and in the solubility where the dielectric discontinuity plays quite a relevant role.⁹⁻¹¹

The remaining of the paper goes as follows. In the section 2 the new model, the KBr/ ϵ , is introduced and the TIP4P/ ϵ water model was reviewed. Section 3 summarizes the simulation details and the results are analysed in Section 4. Conclusions are presented in the section 5.

The Models

The KBr/ ϵ Model

The ions of the salt are modeled as spherical particles interacting through the potential

$$u(r_{ij}) = 4\epsilon_{ij} \left[\left(\frac{\sigma_{ij}}{r_{ij}} \right)^{12} - \left(\frac{\sigma_{ij}}{r_{ij}} \right)^6 \right] + \lambda_i \lambda_j \frac{q_i q_j}{4\pi\epsilon_0 r_{ij}} \quad (1)$$

where r_{ij} is the distance between ions i and j , q_i is the electric charge of ion i , ϵ_0 is the permittivity of vacuum, ϵ_{ij} is the Lennard-Jones energy that is used as energy scale and σ_{ij}

is the distance between the ions, used as length scale.

For the interaction between the ions and the water molecules, the Lorentz-Berteloth rule is employed,¹⁵ namely

$$\sigma_{\alpha\beta} = \left(\frac{\sigma_{\alpha\alpha} + \sigma_{\beta\beta}}{2} \right) ; \quad \epsilon_{\alpha\beta} = \sqrt{\epsilon_{\alpha\alpha}\epsilon_{\beta\beta}} . \quad (2)$$

For the KBr/ ϵ model the Lennard-Jones (LJ) energy, $\epsilon_{ij} = \epsilon_{LJ}$, and the distance scale, $\sigma_{ij} = \sigma_{LJ}$, are the same for any i and j namely K-K, K-Br or Br-Br. The ion charges are $q_i = \pm 1 e$ where e is the charge of an electron.

Recently a new model for the NaCl, the NaCl/ ϵ , was proposed. In this system, a screening for the Coulombic term was introduced.¹⁶ The original assumption was to include effects due to water polarization by adding to a rigid model a screening term.^{8,16} Here we adapt this proposition for the KBr salt model. Then the screening parameter becomes $\lambda_i = \lambda_C$.

Therefore, our interaction potential of the ions has three parameters, namely λ_C , σ_{LJ} and ϵ_{LJ} to be adjusted with experimental data for each ion. These parameters are selected so the KBr/ ϵ force field reproduces the experimental value for the density of the crystal in the face centred cubic phase at the 298 K of temperature^{7,18} and 1 bar. These procedure allows for a number of possible parameters values. This degeneracy is broken by selecting the subset that also gives the radial distribution function, $g(r)$, which gives the appropriate behavior of the salt crystal at 298 K of temperature and 1 bar of pressure.

The next step is this reduction in the parameter space is to select the set of values that also gives the proper density and the dielectric constant in the mixture of the salt with water¹⁸ at 298 K of temperature and 1 bar of pressure. These last step was done using a solution with 4 molal of salt concentration and the TIP4P/ ϵ water model. The final result for the force field for the KBr/ ϵ model is shown in the Table 1.

Table 1: Force field parameter of KBr/ ϵ .

Model	q/e	λ_C	$\sigma/\text{\AA}$	$(\epsilon/k_B)/\text{K}$
K	+1	0.885	2.86	115.83
Br	-1	0.885	4.057	287.47

TIP4P/ ϵ Water Model

The TIP4P/ ϵ ¹² water is illustrated in the figure 1. The intermolecular force is given by the Lennard Jones and the Coulomb interactions as given by the Eq. ???. The positive charges are located at each hydrogen and the negative charge which neutralizes the molecule is placed along the bisector of the HOH angle located at distance l_{OM} of the oxygen as shown in the figure 1. The parameters of the Force Fields for the TIP4P/ ϵ are given in the Table 2 with $\lambda_O = \lambda_H = 1$ in the Eq. ???.

Table 2: Force field parameters of TIP4P/ ϵ water model. The charge in site M is $q_M = -(2q_H)$.

Model	$r_{OH}/\text{\AA}$	$\Theta/^\circ$	q_H/e	q_M/e	$r_{OM}/\text{\AA}$	$\sigma/\text{\AA}$	$(\epsilon/k_B)/\text{K}$
TIP4P/ ϵ	0.9572	104.52	0.527	1.054	0.105	3.165	93

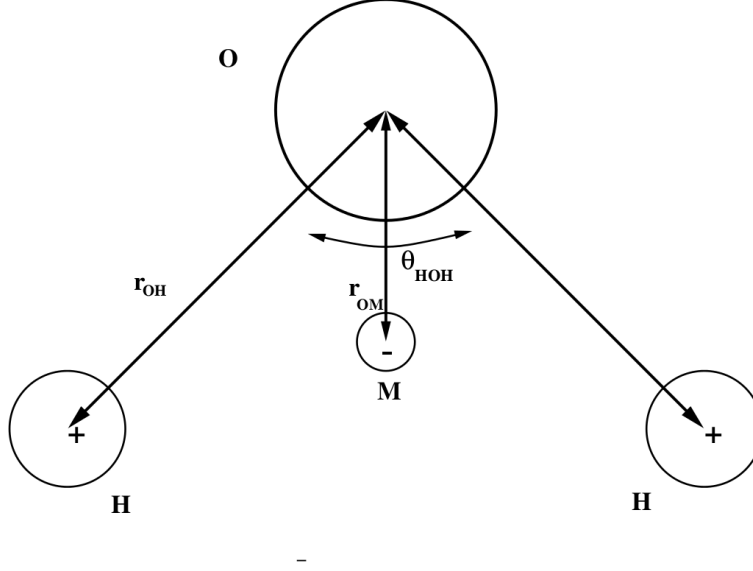


Figure 1: Geometry forcefield of TIP4P/ ϵ water, based on the geometry of the force field TIP4P.²⁰ The geometry have a positive charges on every nucleus of H and a negative charge at a distance r_{OM} along the bisector of the bending angle.

The Simulation Details

Molecular dynamic (MD) simulations were performed using GROMACS.²¹ The equations of motion were solved using the leap-frog algorithm^{21,22} with 2 *fs* time steps. The total time for the simulation for different molalities is 30 ns, keeping the positions and velocities for every 500 steps.

For the shear viscosity shorter times steps and longer simulations were employed, 1 *fs* and 40 ns respectively. The Coulombic forces were treated via Ewald summations with the real part of the Coulombic potential truncated at 10Å. The Fourier component of the Ewald sums was evaluated by using the smooth particle mesh Ewald (SPME) method²³ with a grid spacing of 1.2Å and a fourth degree polynomial for the interpolation. The simulation box is cubic throughout the whole simulation and the geometry of the water molecules kept constant using the LINCS procedure.²⁴ The NpT ensemble was employed with the Nosé Hoover thermostat²⁵ and the Parinell-Rahman barostat with a τ_P parameter of 1.0 ps.²¹

The MD simulations for the pure KBr were carried out under 1 *bar* pressure condition, on a system of 1024 KBr pairs, with a time step $\Delta t = 2$ *fs*, the time of simulations is 10 ns

and storing the positions and velocities every 1000 simulation step. For bromide potassium in water, the simulations have been done using 864 molecules in the liquid phase at different molalities and at the temperature of 298 K and 1 bar of pressure. The molality concentration is obtained from the total number of ions in solution N_{ions} , the number of water molecules N_{H_2O} and the molar mass of water M_{H_2O} as:

$$[KBr] = \frac{N_{ions} \times 10^3}{2N_{H_2O}M_{H_2O}}. \quad (3)$$

The division by 2 in this equation accounts for a pair of ions and $M_{H_2O} = 18 \text{ g mol}^{-1}$. The figure 3 gives the value of the molality for each point of calculus

Table 3: Composition of KBr solutions used in the simulations at 298.15 K and 1 bar.

Molality (m)	N_{H_2O}	N_{ions}
0.99	832	32
1.99	806	58
3.07	778	86
4.05	754	110
5.0	732	132

The static dielectric constant is computed from the fluctuations²⁶ of the total dipole moment \mathbf{M} ,

$$\epsilon = 1 + \frac{4\pi}{3k_BTV}(\langle \mathbf{M}^2 \rangle - \langle \mathbf{M} \rangle^2) \quad (4)$$

where k_B is the Boltzmann constant and T the absolute temperature. The dielectric constant is obtained for long simulations at constant density and temperature or at constant temperature and pressure. The shear viscosity is obtained using the autocorrelation function of the off-diagonal components of the pressure tensor $P_{\alpha\beta}$ according to the Green-Kubo formulation,

$$\eta = \frac{V}{k_BT} \int_0^\infty \langle P_{\alpha\beta}(t_0)P_{\alpha\beta}(t_0+t) \rangle_{t_0} dt, \quad (5)$$

Results

The KBr/ ϵ Model

The parameters for KBr/ ϵ model were selected to reproduce the density of the crystal at the 298 K and 1bar, namely 2.74 g cm^{-3} ¹⁸ and the to show the peak in the radial distribution at 3.29 given in the figure 2 in agreement with the experiments.¹⁸ The final step of the model is obtained by adjusting the parameters to give the correct dielectric constant of the 4 molal solution of the salt in water.

The Lattice Energy (LE) of the KBr/ ϵ model is 582.9 kJ/mol while the Lattice Constant (LC) is 6.58 what is comparable with the experimental data for these two quantities that are given by 671.11 kJ/mol ¹⁸ and by 6.6¹⁸ respectively.

The Table 4 shows a comparison of the values obtained for the the density, the Lattice Energy and the Lattice Crystal for the KBr/ ϵ model, for the experiments,¹⁸ for the Joung-Cheatham,⁷ the **JC** force field, and for the force field parametrized with SPC/E water, the JC_{S3} model.¹⁷ Our model gives good agreement with the experiments¹⁸ in the density of the crystal and the Lattice Constant, but is 13% far from the reproduction of the Lattice Energy.

The figure 3 illustrates the the dielectric constant versus molal concentration for the KBr/ ϵ model with the TIP4P/ ϵ water, for the experiments,¹⁸ JC_{S3}¹⁷ and JC_{T4}⁷ models. The molal concentration employed to parametrize the KBr/ ϵ is shown with a purple circle. The result shows that our model gives a good agreement with the experiments.

In the figure 4 shows the density versus salt concentration for the experiments,¹⁸ for the

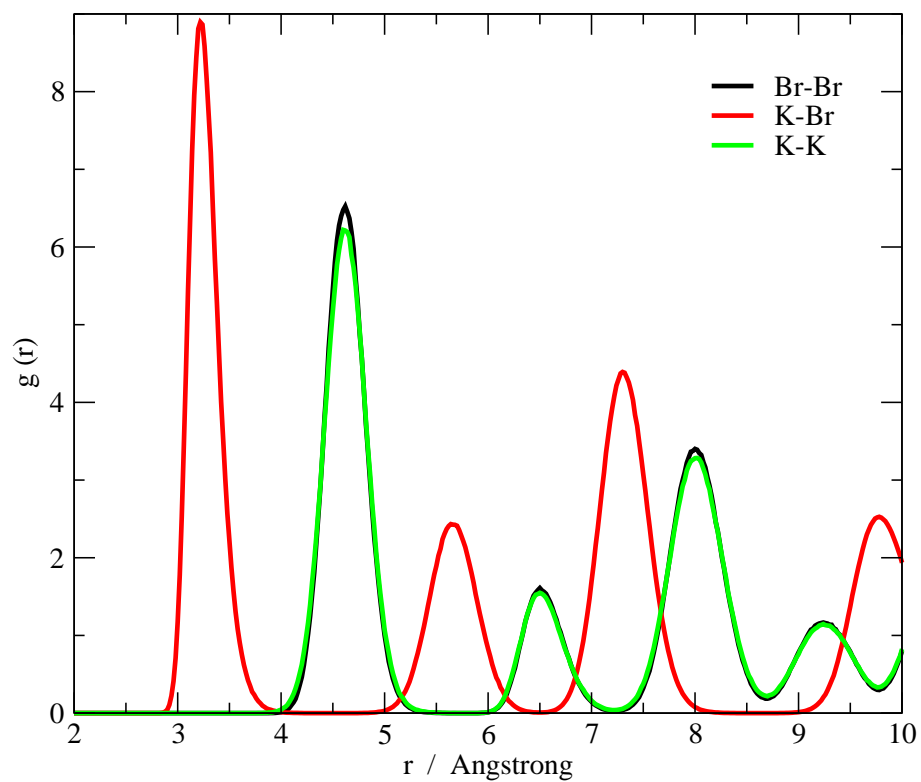


Figure 2: Radial distribution function $g(r)$ versus the distance r at 1 bar and 298 K for: K-Br (red line), K-K (green line), and Br-Br (black line).

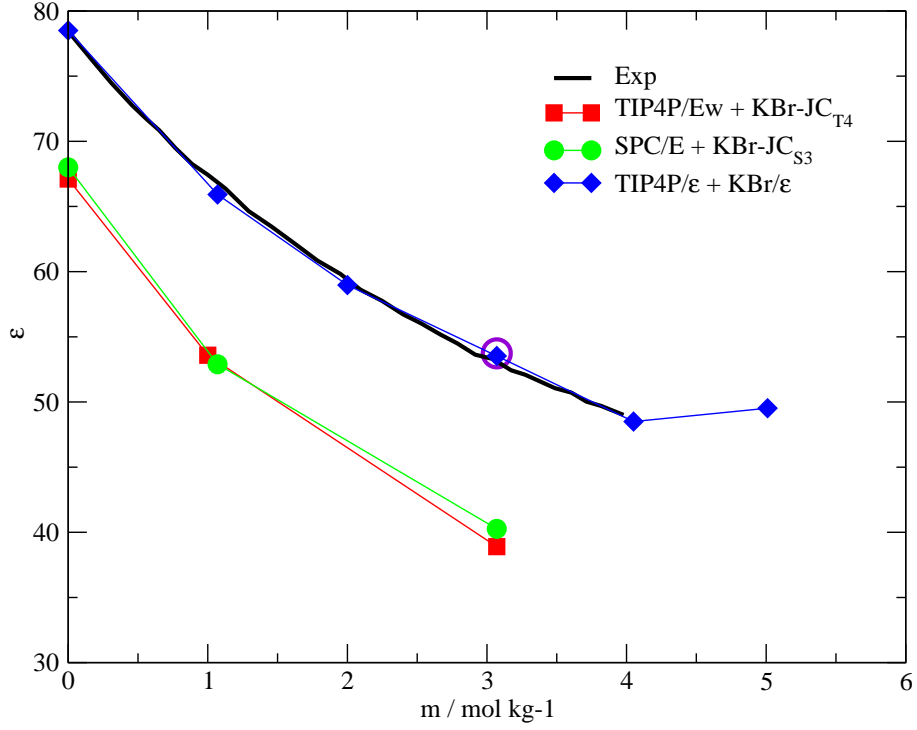


Figure 3: Dielectric constant versus molal concentration of the KBr salt at 1bar and 298 K. The black line is the experimental data,¹⁸ the blue filled diamond is the results for the KBr/ ϵ model , the green spheres are the results for the JC_{S3} model while the red squares are the results for the JC_{T4} model. The violet circle shows the concentration used for the parametrization of the model.

Table 4: Density of KBr at 1 bar of pressure and 298 K of temperature, Lattice Energy, Lattice Crystal of various Force Fields and for experiments.¹⁸

Model Ions	$\rho/(g/cm^3)$	LC/Å	LE/(kJ/mol)
JCS3 ¹⁷	2.61	6.66	695.38
JCT4 ⁷	2.67	6.62	698.72
KBr/ ϵ	2.76	6.58	582.9
experimental ¹⁸	2.74	6.6	671.11

KBr/ ϵ , for the JCS3¹⁷ and for the JCT4⁷ models. The results are consistent with the fact that the models were parametrize to give the correct density value.

In addition to thermodynamic properties, the transport was also evaluated. The shear viscosity η at different molal concentrations at 1 bar and 298 K of pressure and temperature respectively. The figure 5 illustrates the viscosity versus the molal concentration of the salt showing an increase of η as the salt concentration increases what implies that the system becomes more viscous. This result is consistent with the experimental values¹⁸ at diluted concentration also shown in the same figure. When the concentration is increased the agreement with the experiments is lost.

Table 5: Ion-Water Coordination Numbers obtained by our simulations along the r-range used in the integration.

molal concentration	MD KO	MD BrO
3.07	5.38	5.13
5	4.71	4.51

The water coordination numbers around the K and Br ions, 5, can be estimated by integrating the area under the first peak of the K-O and Br-O pair distribution functions up to the first minimum respectively, 6.

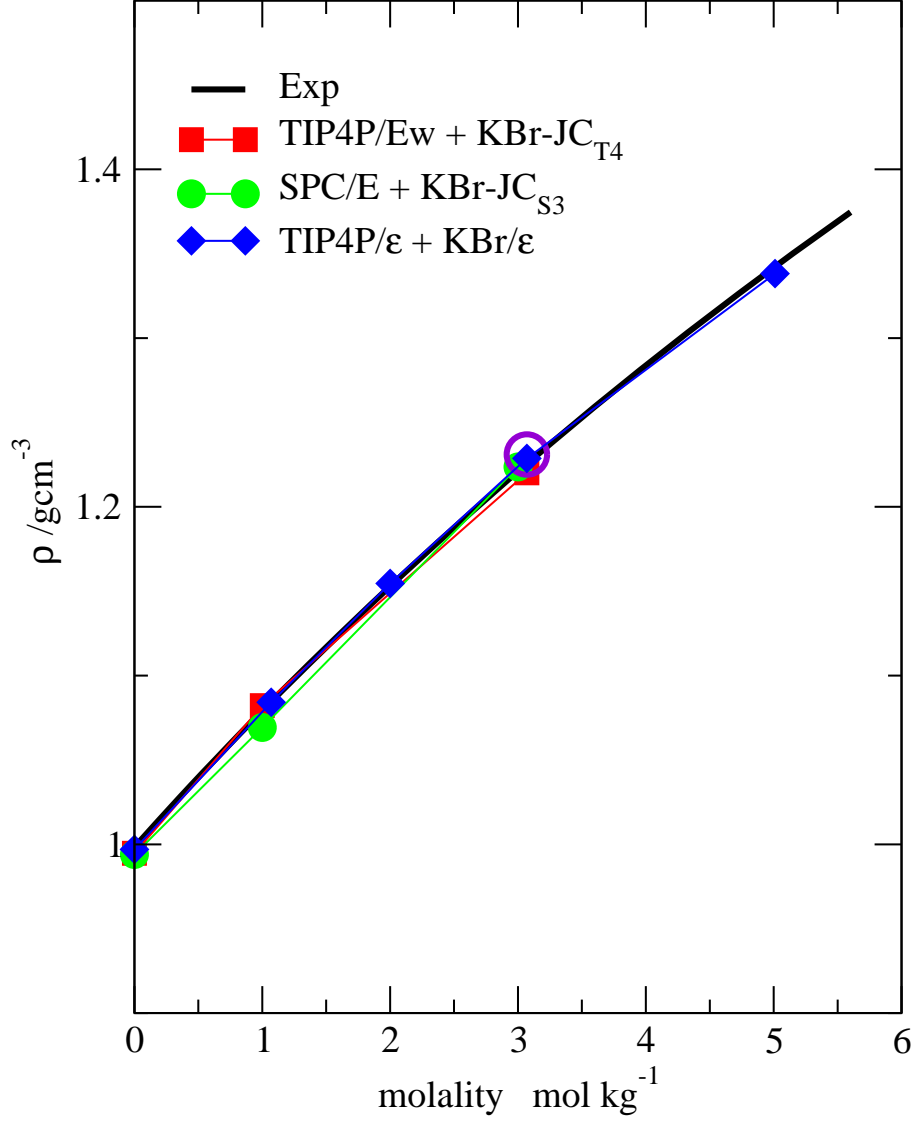


Figure 4: Density versus molal concentration of the salt at 298 K and 1bar. The black line is the experimental data,¹⁸ the blue filled diamond is the results for the KBr/ε model, the green spheres are the results for the JC_{S3} model while the red squares are the results for the JC_{T4} model. All data are at 1bar and 298 K. The iolet circle shows the concentration used for the parametrization of the model.

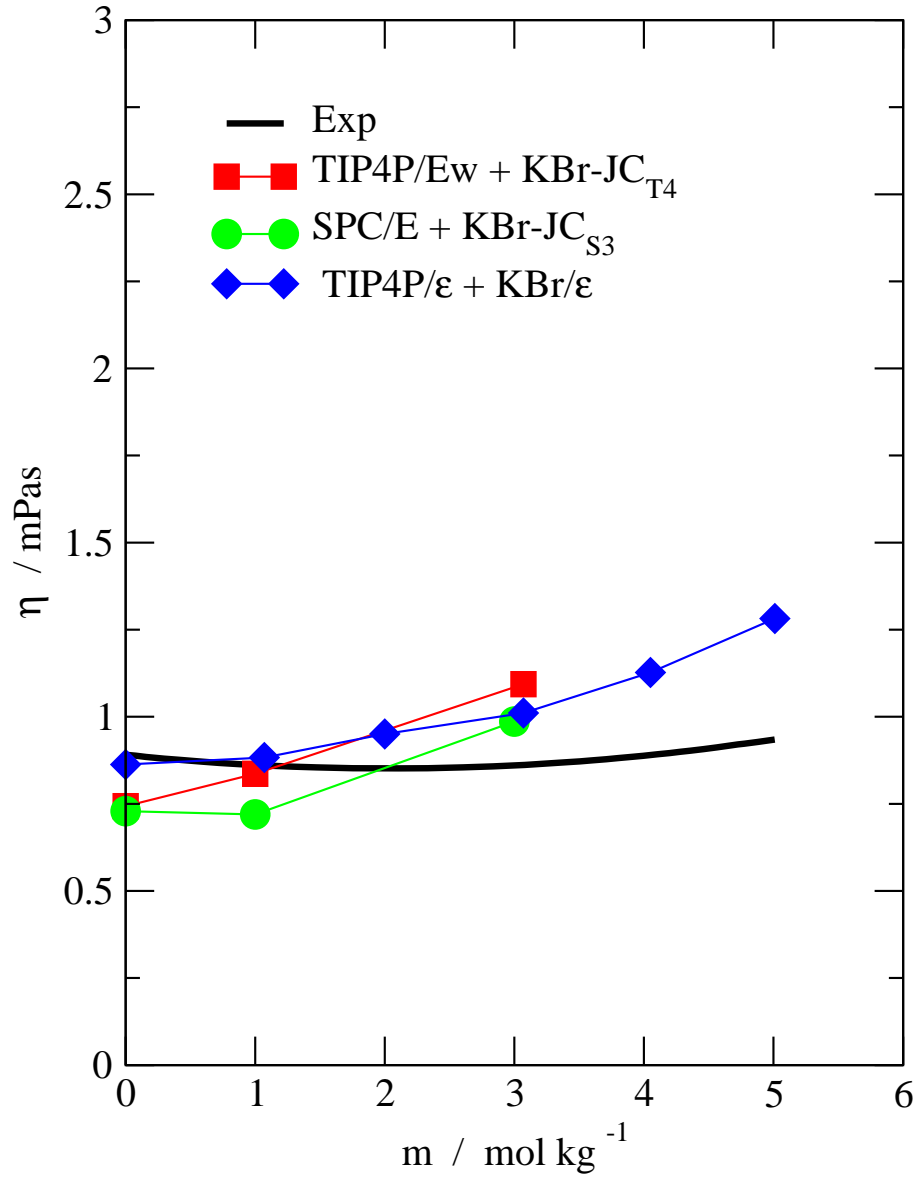


Figure 5: Viscosity versus molal concentration of the salt at 298 K and 1bar. The black line is the experimental data¹⁸ and the blue filled diamond are the results for our model.

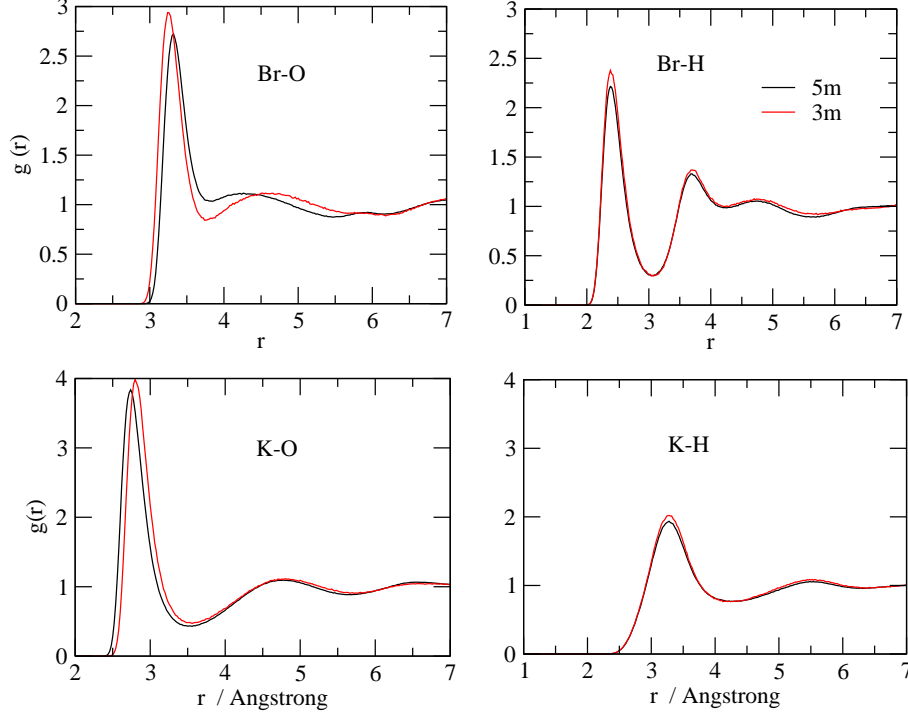


Figure 6: Ion-water pair distribution functions using the rigid water model TIP4P/ ϵ and KBr/ ϵ force field at 298 K, 1 bar, and ionic concentrations of 5 (black line) and 3 (red line) molal. In all cases 864 molecules were used.

The KCl/ ϵ Model

Since both NaCl/ ϵ and KBr/ ϵ models have been already parametrized, we test the transferability of these two force fields as follows. Instead of fitting the parameters for the KCl from experiments, the parameters for the K are taken from the KBr/ ϵ given in the Table 1 while the parameters for the Cl are taken from the NaCl/ ϵ model.⁸ The parameters for the KCl are summarized in the Table 6. It is important to notice that no additional parameterization was needed for obtaining the KCl/ ϵ model.

Table 6: Force field parameter of KCl/ ϵ .

Model	q/e	λ_C	$\sigma/\text{\AA}$	$(\epsilon/k_B)/\text{K}$
K	+1	0.885	2.86	115.83
Cl	-1	0.885	3.85	192.45

First, we test the value of the density of the crystal of KCl/ ϵ at the 298 K and 1 bar

of pressure. Our results give 1.99 g cm^{-3} , that is the same as the experimental data.¹⁸ The radial distribution for K-K, Cl-Cl and K-Cl is illustrated in the Figure 7 and it shows a peak at 3.08 in agreement with the experiments.¹⁸

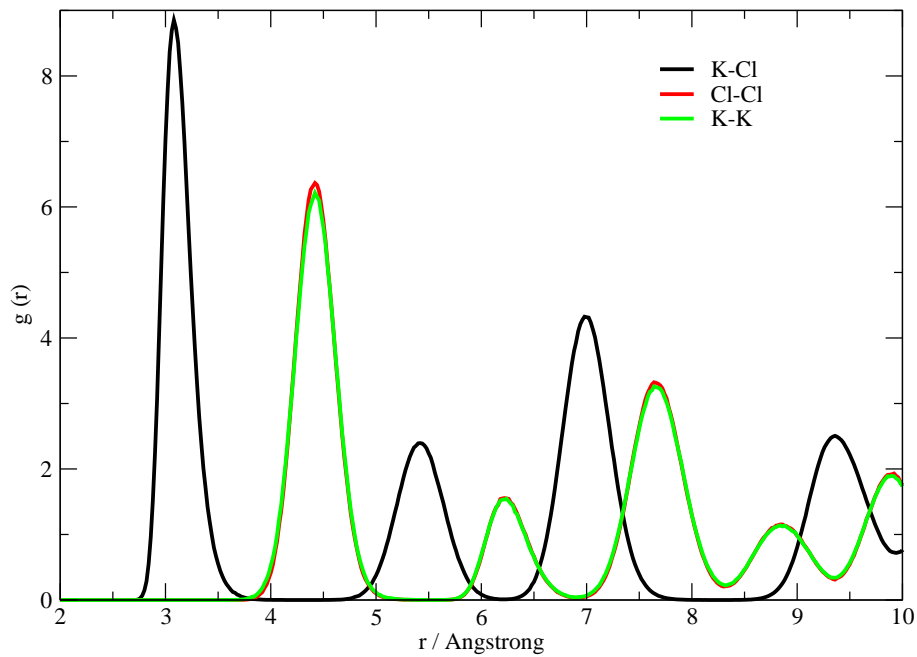


Figure 7: Radial distribution function $g(r)$ versus the distance r at 1 bar and 298 K for: Cl-Cl (red line), K-K (green line), and K-Cl (black line).

The Lattice Constant (LC) at 1 bar of pressure and 298 K of temperature, illustrated in the Table 7, is also in accordance with the experimental values.¹⁸ The Lattice Energy (LE), however, it is 16.5% far from the reproduction of the Lattice Energy. This difference was present in the NaCl/ ϵ and KBr/ ϵ and models.

Table 7: Density of KCl at 1 bar of pressure and 298 K of temperature, Lattice Energy, Lattice Crystal of various force fields and for experiments.¹⁸

Model Ions	$\rho/(g/cm^3)$	LC/Å	LE/(kJ/mol)
JC _{s3} ¹⁷	1.86	6.38	720.9
JC _{T4} ⁷	1.90	6.34	724.6
KBr/ ϵ	1.99	6.29	600.77
experimental ¹⁸	1.99	6.26	720.06

Next, the KCl/ ϵ in the water TIP4P/ ϵ performance is tested for a number of properties. The dielectric constant of the solution as a function of the molal concentrations is shown in the figure 8 giving a good agreement with the experiments.¹⁸ Similarly the figure 9 gives the density at a function of the molal concentration of KCl.

The shear viscosity η at different molal concentrations at 1 bar and 298K is shown in the figure 10 showing a good agreement with the experiments.

Using the radial distribution functions respect to oxygen of the cation and anion at different concentrations. We calculated the number of coordination around the K and Cl, we do this through the integration the area under the first peak of the K-O and Cl-O pair distribution functions up to the first minimum respectively, 11. These coordination numbers are shown in the table 8 and give a good agreement with the experiments in the case of KO.

The NaBr/ ϵ Model

The consistency of the new force fields is now checked by creating the NaBr/ ϵ model employing the parameters for Br and Na, shown in the table 9, extracted from the force fields for the KBr/ ϵ and NaCl/ ϵ models respectively. The radial distribution for Na-Na, Br-Br

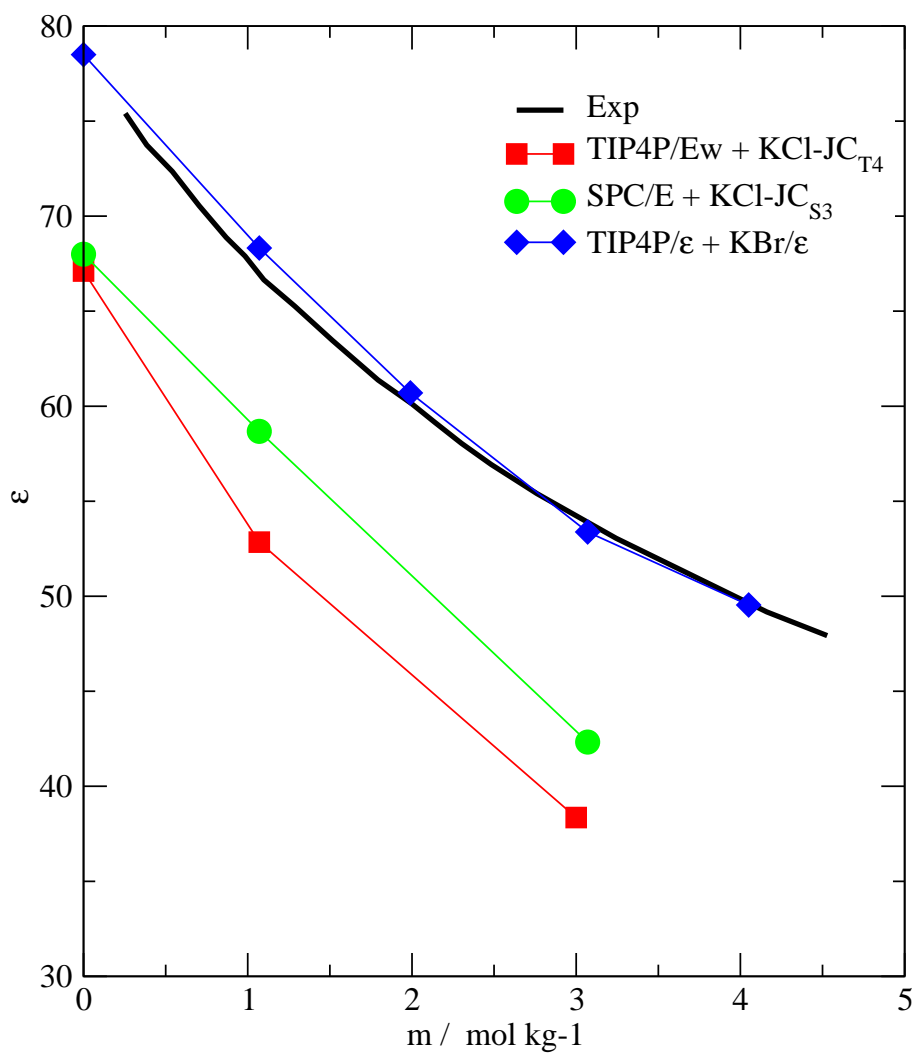


Figure 8: Dielectric constant versus molal concentration of the salt at 298 K and 1bar . The black line is the experimental data¹⁸ and the blue filled diamond is the results of our model. All data are at room conditions.

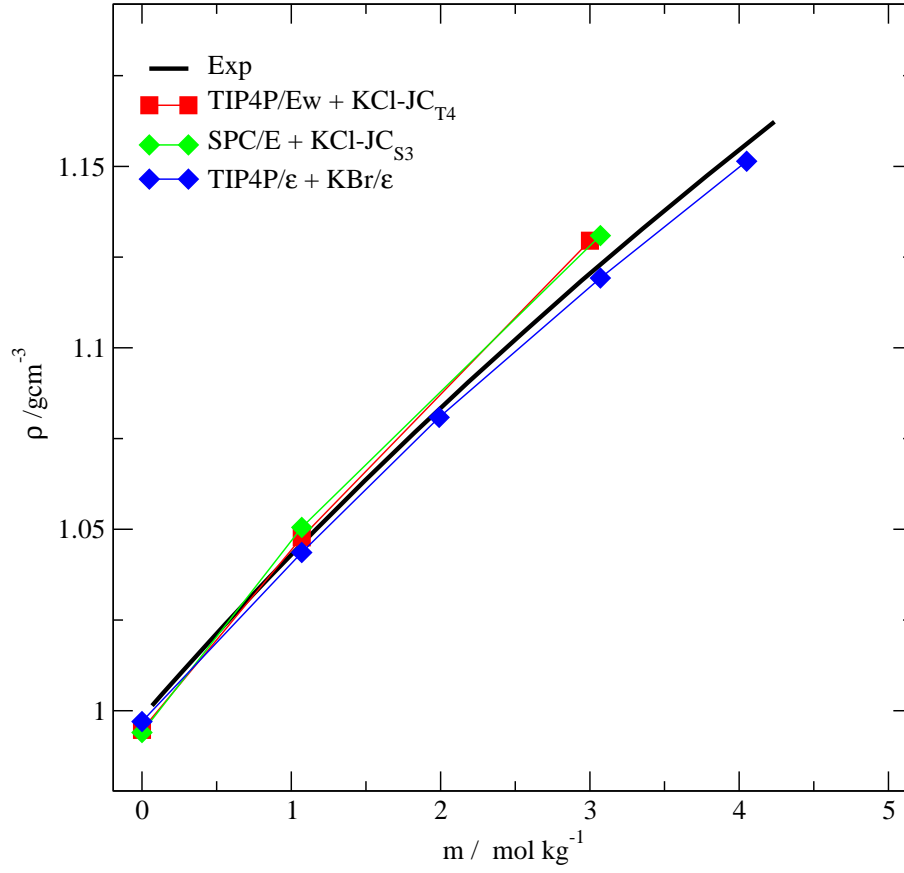


Figure 9: Density versus molal concentration of the salt at 298 K and 1bar. The black line is the experimental data¹⁸ and the blue filled diamond are the results of our model.

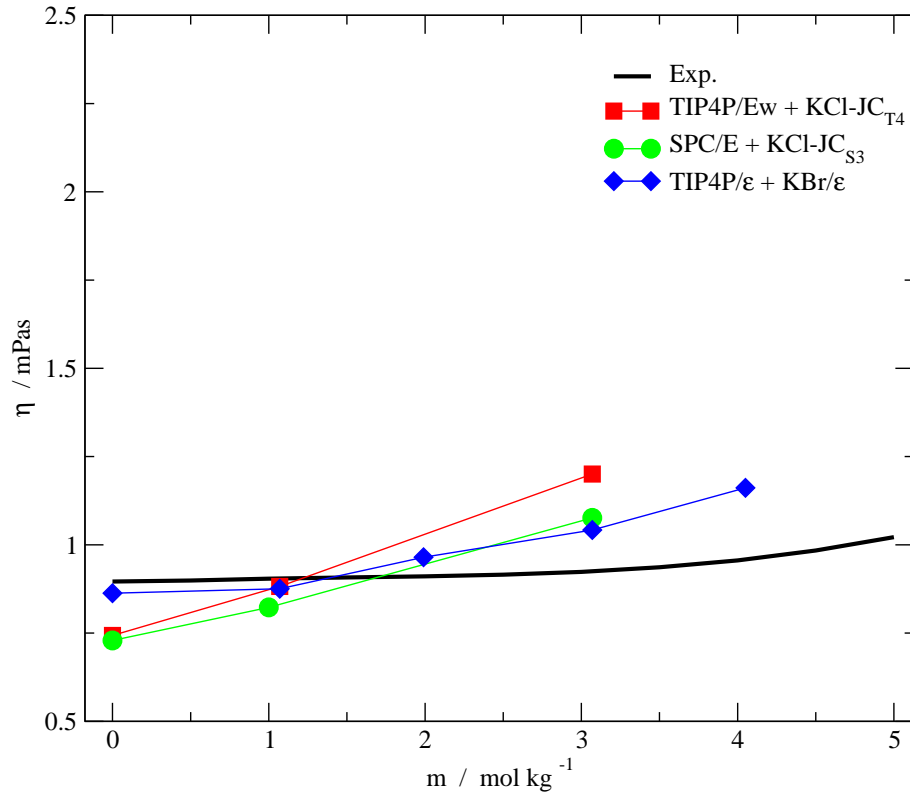


Figure 10: Viscosity versus molal concentration of the salt at temperature and pressure at room conditions. The black line is the experimental data¹⁸ and the blue filled diamond are the results for our model.

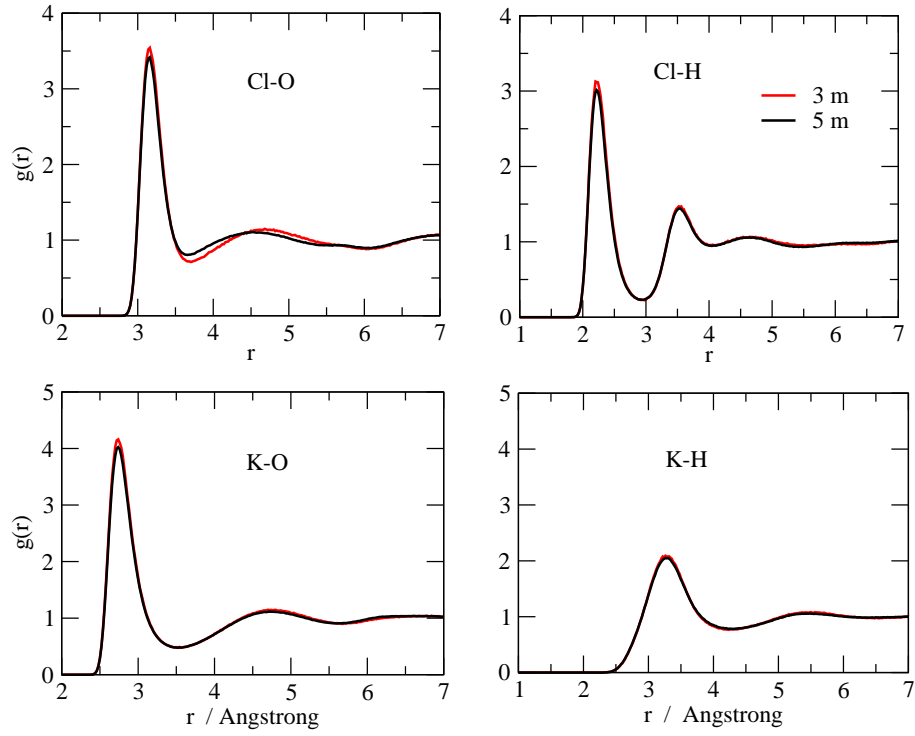


Figure 11: Ion-water pair distribution functions using the rigid water model TIP4P/ ϵ and KCl/ ϵ force field at 298 K, 1 bar, and ionic concentrations of 5 (black line) and 3 (red line) molal. In all cases 864 molecules were used.

Table 8: Ion-Water Coordination Numbers obtained by our simulations and experiments. The uncertainties of experimental data¹⁹ are reported within parenthesis, along with the r-range used in the integration.

molal concentration	MD KO	MD ClO	Exp ²⁸ KO
3.07	5.61	5.46	5.7
5	5.18	5.10	5.1

and Na-Br are illustrated in the figure 12. The density of the crystal, the lattice energy and the lattice constant are shown in the table tab:FFcompNaBr showing a good agreement with the experimental results.

Table 9: Force field parameter of NaBr/ ϵ .

Model	q/e	λ_C	$\sigma/\text{\AA}$	$(\epsilon/k_B)/\text{K}$
Na	+1	0.885	2.52	17.44
Br	-1	0.885	4.057	287.47

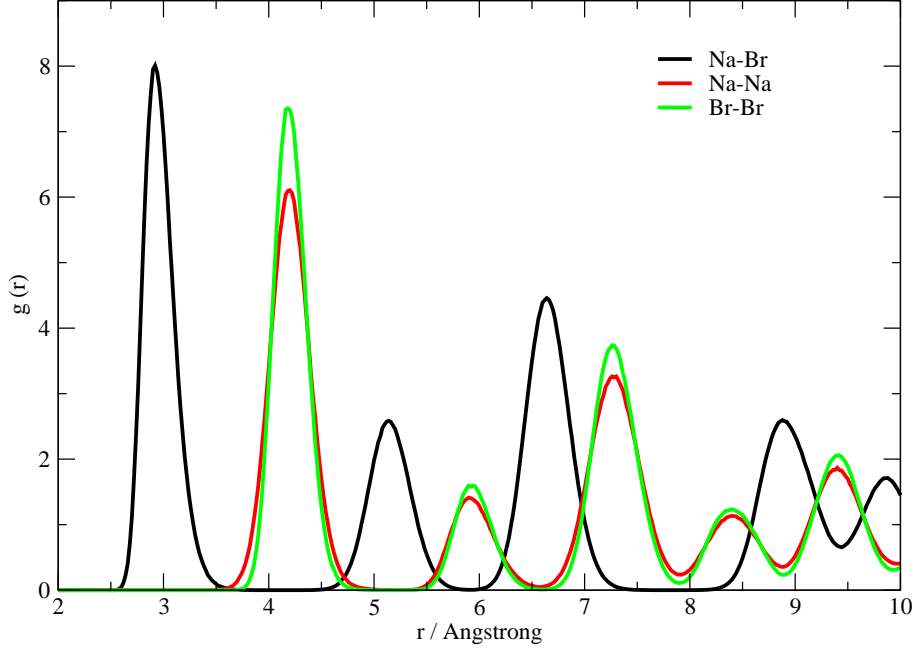


Figure 12: Radial distribution function $g(r)$ versus the distance r at 1 bar and 298 K for: Na-Na (red line), Br-Br (green line), and Na-Br (black line).

Table 10: Density of NaBr at 1 bar of pressure and 298 K of temperature, Lattice Energy, Lattice Crystal of various force fields and for experiments.¹⁸

Model Ions	$\rho/(g/cm^3)$	LC/Å	LE/(kJ/mol)
JC _{s3} ¹⁷	3.00	6.06	761.48
JC _{T4} ⁷	3.09	6.00	766.50
NaBr/ ϵ	3.2	5.90	600.77
experimental ¹⁸	3.2	5.97	753.95

The figure 13 illustrates the dielectric constant versus molal concentration of the NaBr/ ϵ salt model in solution with the TIP4P/ ϵ water. The graphs shows that the new model gives a better agreement with the experiments than the other atomistic parameterizations.

The density of the NaBr/ ϵ with the TIP4P/ ϵ water at various concentrations is show in the figure 14. These force fields reproduce the density of the diluted solution very well and when the solution increases in concentration we see that the value the same with respect to experimental, so in a 6m solution we find that the value of the JC_{S3} is 1.5 percent and the JC_{T4} is 1.6 percent diferent with respect to the experimental.

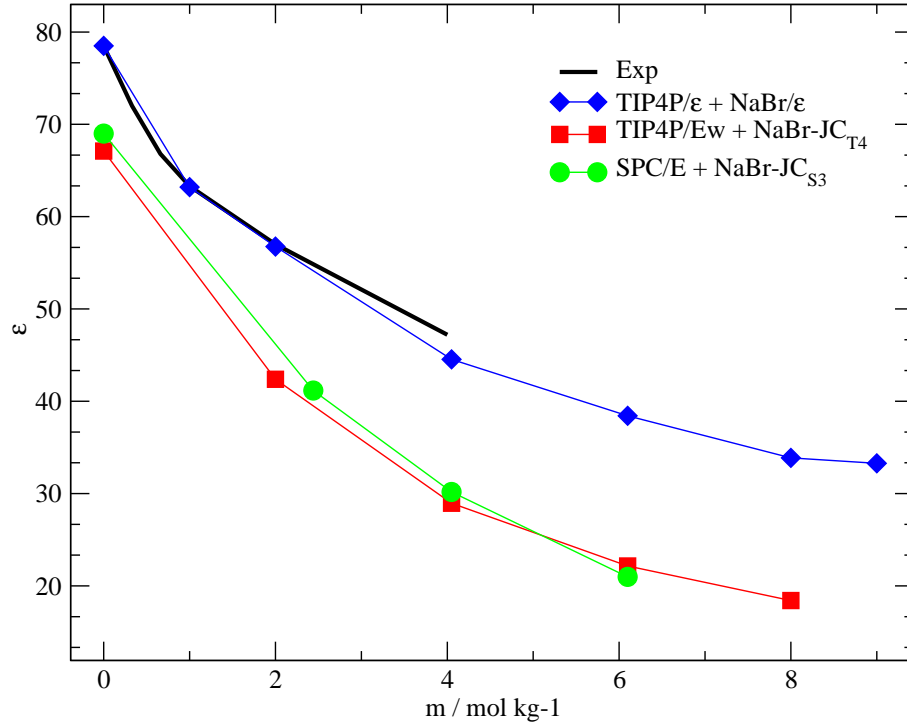


Figure 13: Dielectric constant versus molal concentration of the salt. The black line is the experimental data¹⁸ and the blue filled diamond is the results of our model. All data are at room conditions. Violet circle is the diluted concentration where was made the parameterization.

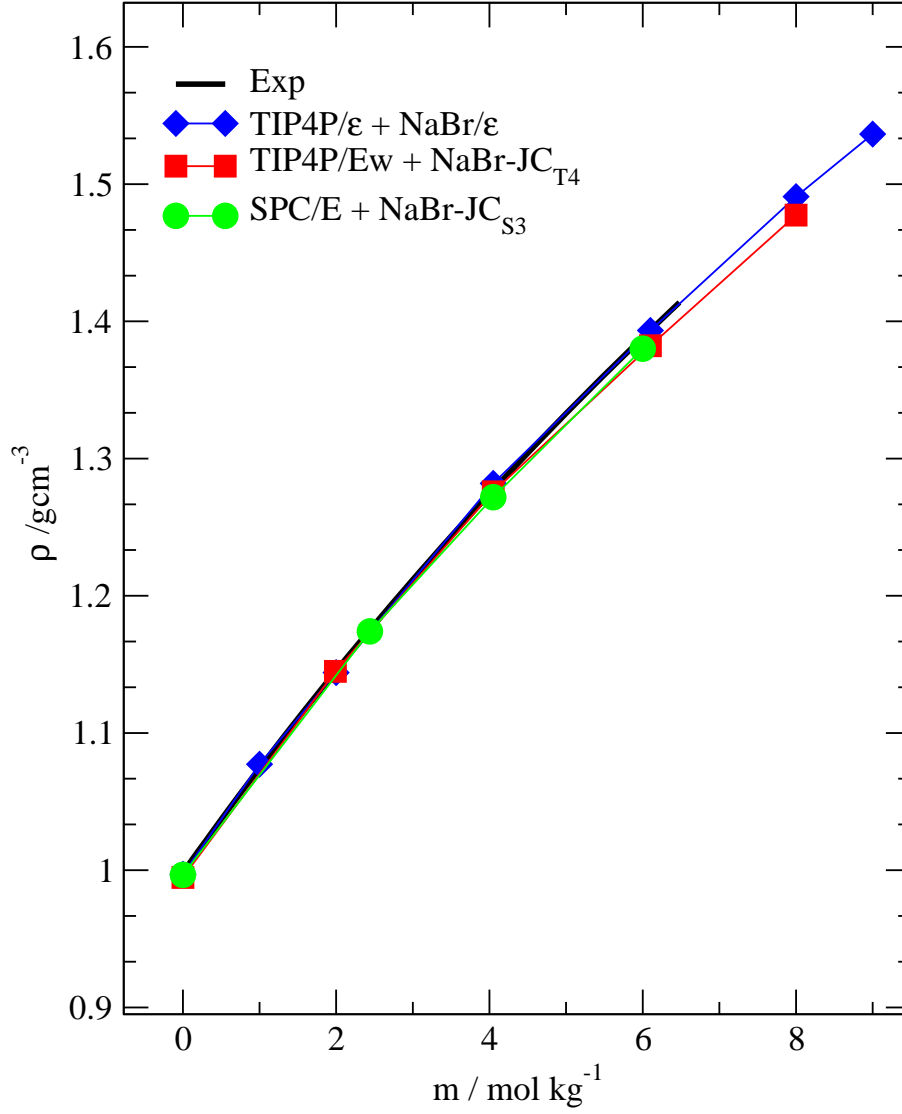


Figure 14: Density versus molal concentration of the salt at 298 K and pressure. The black line is the experimental data¹⁸ and the blue filled diamond are the results of our model. Violet circle is the diluted concentration where was made the parameterization.

The calculus of the shear viscosity η at different molal concentrations at 1 bar and 298K of pressure and temperature respectively, 15 show the shear viscosity versus molal concentration of the salt showing an increase of η as the salt concentration increases what implies that the system becomes more viscous. This result is consistent with the experimental values¹⁸ at diluted concentration also shown in the figure. When the concentration is increase there is a difference between the value that reproduces the NaBr/ ϵ with TIP4P/ ϵ of 13.5% at 6.1m, compared to experimental value and the JC_{S3} with respect to the experimental value is 55.3 percent and the JC_{T4} is 71.4 percent at the same experimental concentration of 6.1m. It is important to note that the result with the new force field NaBr/ ϵ describes the curvature of the shear viscosity.

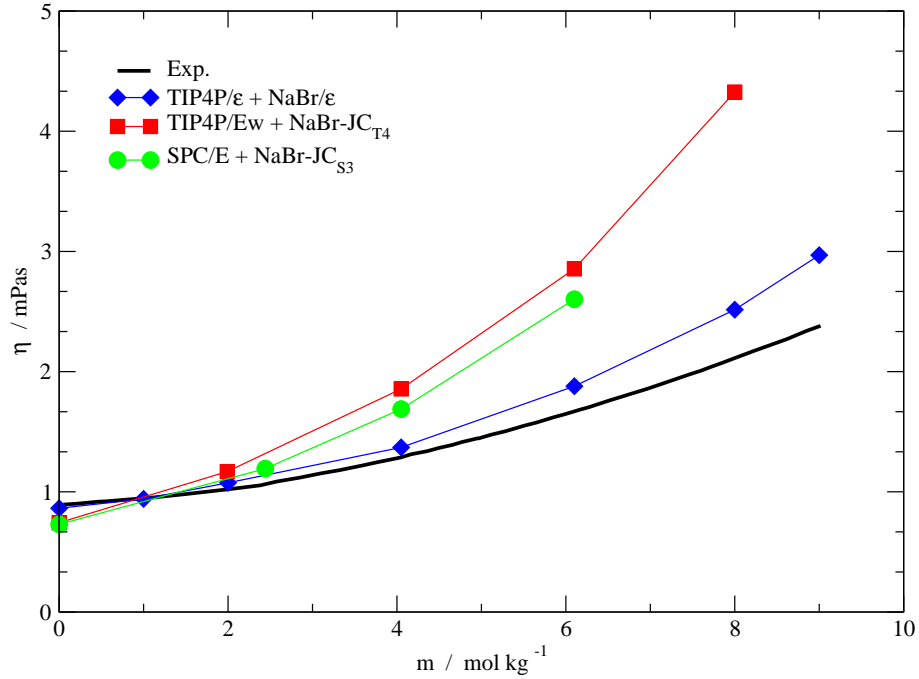


Figure 15: Viscosity versus molal concentration of the salt at temperature and pressure at room conditions. The black line is the experimental data¹⁸ and the blue filled diamond are the results for our model.

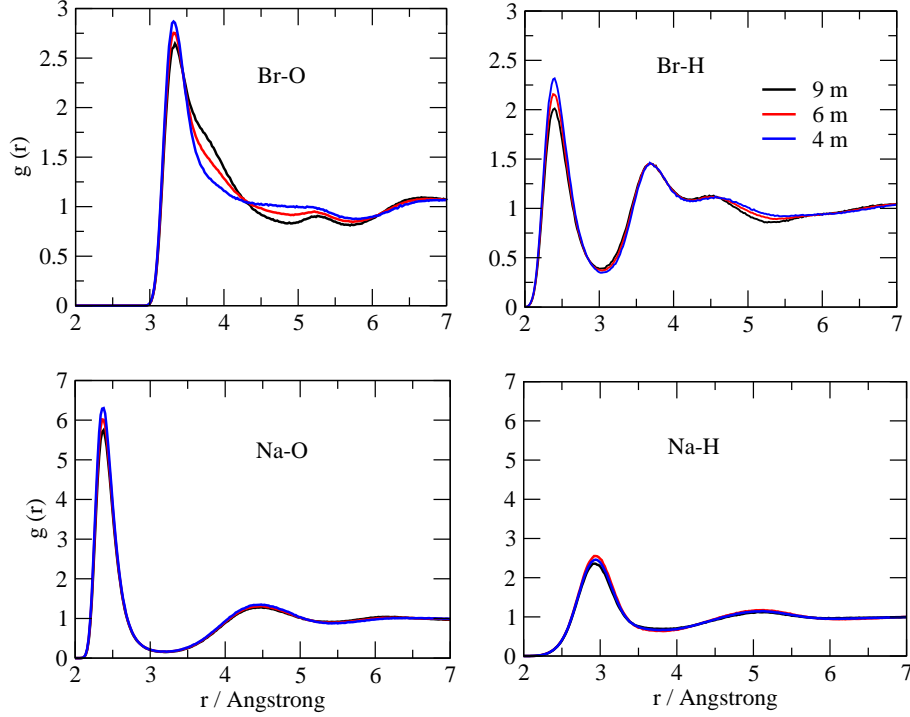


Figure 16: The radial distribution function for (a) Br-O, (b) Br-H, (c) Na-O and (d) Na-H in TIP4P/ ϵ water with NaBr/ ϵ at salt concentrations of 9 (black line), 6 (red line) and 4 (blue line) molal. In all cases 864 molecules were employed.

The ion-water radial distribution functions are illustrated in the figure 16. Employing this functions, the coordination around the NA and Br were computed and shown in the table 11.

Table 11: Ion-Water Coordination Numbers obtained by our simulations.

molal concentration	MD NaO	MD BrO
4	4.62	13.8
6	4.14	14.11
9	3.65	12.86

In the figure 17 the solubilities of the new force fields KBr/ ϵ , KCl/ ϵ and NaBr/ ϵ are shown indicating a good agreement with the experiments. The solubility was computed employing method number four from the reference by Manzanilla-Granados et al.²⁹

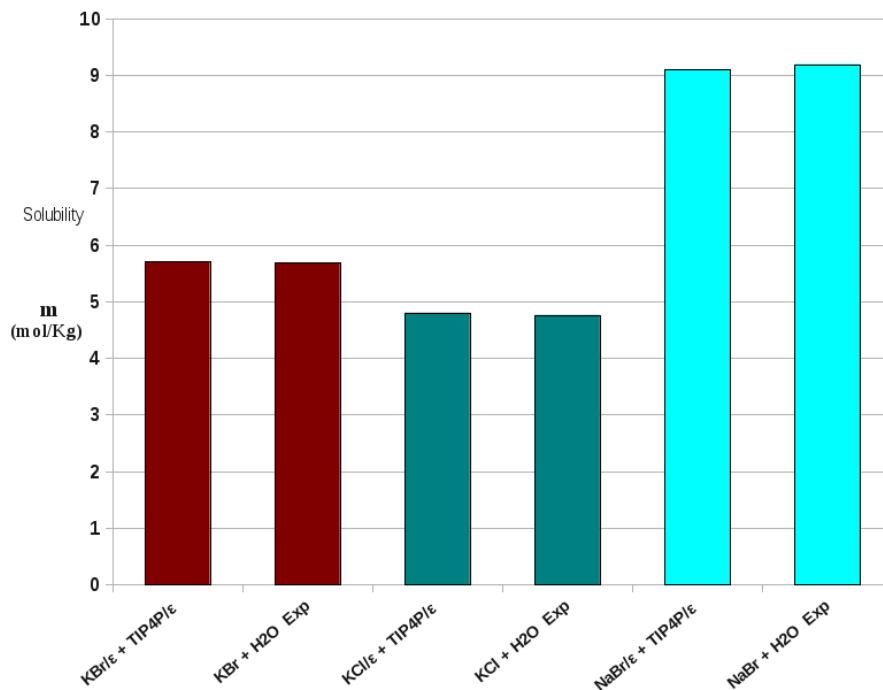


Figure 17: Solubility of the atomistic models

Conclusions

In this paper the force field, the KBr/ ϵ , was introduced. The model reproduces the density of the crystal and structure, as well as the thermodynamic and dynamic properties of the solution with the TIP4P/ ϵ model for water at different molal concentration.

The model, particularly reproduces the dielectric constant of the solution what is a property not well represented in other atomistic models. In order to test the KBr/ ϵ and the NaCl/ ϵ models, the same parameters for the isolated ions were employed in the construction of the KCl/ ϵ and of the NaBr/ ϵ models. In the construction of these two new models not there was an additional parameterization. The results of the density, the dielectric constant, the viscosity and the solubility of the KCl/ ϵ and of the NaBr/ ϵ models reproduces well the experiments. Since all the models give a very robust result for the dielectric constant, we believe that they are suitable for studying confined systems and can be used to study ionic channels.

Acknowledgements

We thank the Brazilian agencies CNPq, INCT-FCx, and Capes for the financial support. We also thank the SECITI of Mexico city for financial support.

R.F.A. thanks José Alejandro Ramirez chief of the Chemistry Department at UAM-Iztapalapa in Mexico city for all the advice and helpful discussions.

References

- (1) I.D. Weiner, S. Linus and C.S. Wingo. in *Comprehensive Clinical Nephrology*, 4th Edition, edited by R. Johnson, J. Fluege and J. Feehally. Saunders Elsevier, 2010, pp 118-129.
- (2) G. Malnic, G. Giebisch, S. Muto, W. Wang, M.A. Bailey, L.M. Satlin. In *physiology and pathophysiology. 5th ed.* edited by R.J. Alpern, M.J. Caplan, O.W. Moe, (Seldin and Giebisch's the kidney: London: Academic Press, 2013) pp. 1659-1716.
- (3) D.B. Mount, K. Zandi-Nejad. Disorders of potassium balance. in *BRENNER & RECTOR'S THE KIDNEY*, 2007. 9th Ed. Elsevier. pp. 640-672.
- (4) A.S. McCall, C.F. Cummings, G. Bhavé, R. Vanacore, Cell **157**, 1380(2014).
- (5) A.N. Mayeno, A.J. Curran, R.L. Roberts, C.S. Foote. J. Biol. Chem. **264**, 5660(1989).
- (6) M.P. Patricelli, J.E. Patterson, D.L. Boger, B.F. Cravatt. Bioorg. Med. Chem. Lett. **8**, 613(1998).
- (7) I.S. Joung, T.E. Cheatham III. J. Phys. Chem. B. **112**, 9020(2008).
- (8) R. Fuentes-Azcatl, M.C. Barbosa. J. Phys. Chem. B. **120**, 2460(2016).
- (9) E. Sanz, C. Vega. J. Chem. Phys. **126**, 014507(2007).
- (10) D. Corradini, M. Rovere, P. Gallo. J. Chem. Phys. **132**, 134508(2010),

- (11) Y. Liu, T. Lafitte, A.Z. Panagiotopoulos, P.G. Debenedetti. *AIChE J.* **59**, 3514(2013).
- (12) R. Fuentes-Azcatl, J. Alejandre. *J. Phys. Chem. B.* **118**, 1263(2014).
- (13) R. Fuentes-Azcatl, M.C. Barbosa. *J. Physica A.* **444**, 86(2016).
- (14) C. Vega, J.L. Abascal. *Phys. Chem. Chem. Phys.* **13**, 19663(2011).
- (15) J. P. Hansen and I. R. McDonald, in *Theory of Simple Liquids*, 3rd ed. Academic, Amsterdam, 2006
- (16) I.V. Leontyev, A.A. Stuchebrukhov. *J. Chem. Phys.* **141**, 014103(2014).
- (17) D.E. Smith, L.X. Dang. *J. Chem. Phys.* **100**, 3757(1994).
- (18) D.R. Lide. IN *CRC Handbook of Chemistry and Physics*, 90 th ed.; CRC Press: Cleveland, OH, USA, 2009.
- (19) R. Mancinelli, A. Botti, F. Bruni, M.A. Ricci, A. K. Soper. *J. Phys. Chem. B* **111**, 13570(2007).
- (20) W.L. Jorgensen, J. Chandrasekhar, J.D. Madura, R.W. Impey, M.L. Klein. *J. Chem. Phys.* **79**, 926(1983).
- (21) M.J. Abraham, D. van der Spoel, E. Lindahl, B. Hess. GROMACS development team. GROMACS User Manual version 5.0, *www.gromacs.org*, (2014).
- (22) M.P. Allen, D.J. Tildesley. in *Computer Simulation of Liquids*, Oxford University Press: Oxford, U.K., 1987.
- (23) U. Essmann, L. Perera, M.L. Berkowitz, T. Darden, H. Lee, L.G. Pedersen. *J. Chem. phys.* **103**, 857(1995).
- (24) B. Hess, H. Bekker, H.J.C. Berendsen, J.G.E.M. Fraaije. *J. Comput. Chem.* **18**, 1463(1997).

- (25) M.E. Tuckerman, Y. Liu, G. Ciccotti, G.J. Martyna. J. Chem. Phys. **115**, 1678(2001).
- (26) M. Neumann. Molec. Phys. **50**, 841(1983).
- (27) K.P. Jensen, W.L.J. Jorgensen. Chem. Theory Comput. **2**, 1499(2006).
- (28) M. Yizhak, Chemical Reviews **88**, 1475(1988).
- (29) H. Manzanilla-Granados, H. Saint-Martin, R. Fuentes-Azcatl, J. Alejandro. J. Phys. Chem.B. **119**, 8389(2015).